ACS OMEGA

http://pubs.acs.org/journal/acsodf

Article

In Situ Assembled Polynuclear Zinc Oxo Clusters Using Modified Schiff Bases as Ligands

Suman Mondal, Smruti Prangya Behera, Mohammed Alamgir, and Viswanathan Baskar*

Cite This: *ACS Omega* 2022, 7, 1090−1099

Read Online

ACCESS | Metrics & More | Article Recommendations | Supporting Information

ABSTRACT: A series of different cores and nuclearity zinc metal clusters **1**−**5** have been synthesized using $Zn(ClO_4)_2{\cdot}6H_2O$, Schiff-base primary ligands, and dibenzoyl methane (DBM) or monoethanolamine (MEA) as co-ligand in a room-temperature reaction. The structure of the complexes is characterized using single-crystal X-ray diffraction. Among them, (**1**) $[Zn(L1)(DBM)]$ is mononuclear; (**2**) $[Zn_4(L2)_2(DBM)_4]$, (**3**) $[Zn_4(L2)_4(H_2O)_2(ClO_4)_2]{\cdot}2CH_2Cl_2$, and (**4**) $[Zn_4(L3)_2(DBM)_4]$ have a cubane core; and (**5**) $[Zn_4(L4)_4(MEA)_2(ClO_4)_2]$ has a ladderlike core structure. Compounds **1**−**5** have also been characterized using UV−vis absorption and emission spectroscopies. For an in-depth understanding of the absorption spectra of **1** and **3**, density functional theory (DFT) calculations have been performed, which suggest that the transitions correspond to the $\pi \rightarrow \pi^*$ intraligand charge transfer (ILCT) transitions.

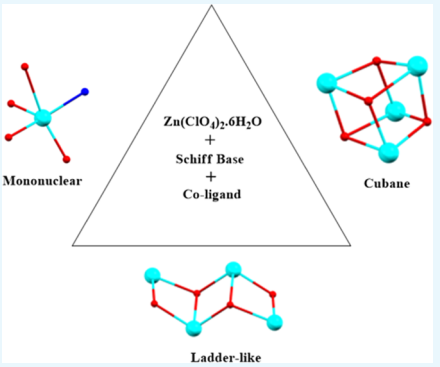

INTRODUCTION

Multicomponent reactions of 3d and 4f elements with multidentate organic/main group elements based on ligands containing donating heteroatoms have been exploited in detail due to their interesting and complex coordination behaviors.[1] Our interest in this area has been established from a series of multinuclear clusters using phosphinate/phosphonate- and organostibonate-based ligand systems that have yielded structurally fascinating molecular clusters of transition metal ions[2] and lanthanides,[3] some of which have shown interesting magnetic properties such as single-molecule magnet (SMM) behavior.[4] We have recently shown the assembly of titanium-based multinuclear clusters, one of which shows interesting structural properties such as fluxional behavior at room temperature.[5] Moreover, we have also recently shown a designed approach for reducing band gaps by synthesizing Ti_4Sb_2-based heteronuclear clusters from a parent Sb_6 molecular framework using solvothermal reaction conditions.[6] We have also been using multidentate donating ligands such as Schiff-base ligands due to their adjustable coordination properties and flexible bridging modes.[7] Using Schiff base/modified vanillin-based Schiff bases, several multinuclear complexes of d/f block elements have been reported.[8] Notable reports among them are multinuclear dysprosium-based clusters reported by Murugesu et al., who synthesized a series of tetranuclear butterfly core-containing dysprosium clusters, and the magnetic measurements revealed that some of these clusters displayed a high energy barrier for reversal of magnetization.[9] In this backdrop, Schiff-base ligands have been used for synthesizing zinc-based multinuclear clusters, some of which have shown interesting applications as polymerization catalysts,[10] reagents in organic synthesis,[11] molecular precursors for ZnO-based materials,[12] models of the active site in zinc enzymes,[13] and in synthesizing functional molecule-based materials.[14] Some of the molecular clusters of zinc reported in the literature are mononuclear,[15] binuclear,[16] trinuclear,[17] tetranuclear,[18] and polynuclear clusters.[19] Some of these structural forms, like the tetranuclear core cluster, have garnered special attention, particularly the manganese-based tetranuclear clusters, which have been involved in multi-electron-transfer redox reactions of oxygen-evolving complex (OEC) of PSII in green plants.[20]

Herein, the synthesis and structural characterization of a series of zinc-based molecular clusters have been reported. By systematically carrying out reactions of metal perchlorates in the presence/absence of the co-ligand used and varying the length of the methylene side chain incorporated in the modified Schiff bases used, different nuclearity-based zinc clusters have been synthesized and structurally characterized. Density functional theory (DFT) calculations have been performed to understand better the electronic absorption spectra of clusters **1** and **3**. The details of the study are presented herein.

Received: October 11, 2021
Accepted: December 8, 2021
Published: December 23, 2021

https://doi.org/10.1021/acsomega.1c05673
ACS Omega 2022, 7, 1090−1099

Scheme 1. Synthesis of Zinc Schiff Base Complexes 1−5

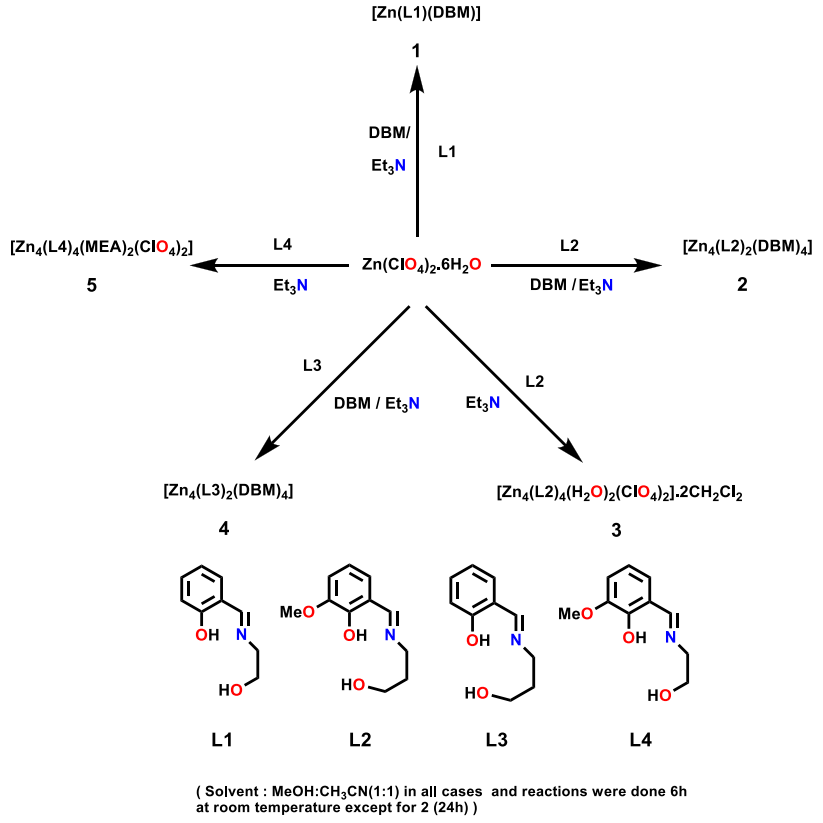

RESULTS AND DISCUSSION

The complexes **1**−**5** were synthesized as summarized in Scheme 1. In these reactions, different chain lengths containing Schiff-base ligands have been employed with (**1**, **2**, **4**, **5**) and without (**3**) auxiliary ligands such as dibenzoyl methane (DBM)/monoethanolamine(MEA) in a mix-solvent methanol−acetonitrile (1:1) medium and triethylamine as a base. All of the Schiff-base ligands L1, L2, L3, and L4 were prepared in an in situ reaction. Ligands L1 and L3 have two oxygen and one nitrogen (O_2N) as a coordinating group, and ligands L2 and L4 have three oxygen and one nitrogen (O_3N) as a coordinating group. Hence, these diprotic (L1, L2, L3, L4) ligands have multiple pairs of electrons to form coordination complexes where ligands can bind between metal atoms as a chelating or bridging mode (Table S2). We report the synthesis and structural characterization of mononuclear and tetranuclear (cube, ladderlike) coordination complexes using these Schiff-base ligands and co-ligands as mixed ligand systems.

Synthesis Procedure Followed for Synthesizing These Complexes Is Detailed Below. In all of the cases, ligands and co-ligands were taken in a solvent mixture (methanol−acetonitrile), and a metal salt (zinc perchlorate hexahydrate) was added followed by dropwise addition of triethylamine base and left for 6 h under stirring, except for **2**, which was stirred for 24 h. The following ligands and co-ligands were used for synthesis. For **1**, salicylaldehyde, monoethanolamine (MEA), and DBM; **2**, *o*-vanillin, 3-aminopropanol, and DBM; **3**, *o*-vanillin and 3-aminopropanol; for **4**, salicylaldehyde, 3-aminopropanol, and DBM; and for **5**, *o*-vanillin and ethanolamine. Different methods are used for crystallization as described. **1** was synthesized by stirring ethanolamine, salicylaldehyde, dibenzoyl methane (DBM), zinc perchlorate hexahydrate, and triethylamine in a 1:1:1:1:3 molar ratio in a methanol−acetonitrile (1:1) solvent mixture for 6 h (Scheme 1). The clear yellowish solution was filtered and the volume was reduced to half. Yellowish rod-shaped crystals were obtained overnight. **2** was synthesized by stirring 3-aminopropanol, *o*-vanillin, DBM, zinc perchlorate hexahydrate, and triethylamine in a 1:1:1:1:3 molar ratio in a methanol−acetonitrile (1:1) solvent mixture for 24 h to maximize the yield of the product (Scheme 1). In the yellow solution, a white precipitate was observed. The precipitate was filtered and dried. Compound **2** was obtained by the chloroform/hexane diffusion method as white crystals in a week's time. **3** was synthesized in the same as **2**, only here DBM was not used. A clear yellowish solution was observed at the end of the reaction, which was filtered and evaporated. After evaporating the solvent, the sticky, oily liquid was dissolved in DCM, and diffusing hexane yielded crystals of **3** within 2 weeks. Compound **4** was synthesized in the same as compound **2**, the difference being salicylaldehyde was used instead of *o*-vanillin. Crystals were obtained by the DCM/hexane layering method at 0 °C. Compound **5** was synthesized by stirring *o*-vanillin, monoethanolamine, zinc perchlorate hexahydrate, and triethylamine in a 1:1.5:1:3 molar ratio in a methanol−acetonitrile (1:1) solvent mixture for 6 h. The clear yellowish solution was filtered and evaporated. From DCM/hexane layering at 0 °C, we obtained X-ray quality crystals.

All of the compounds (**1**−**5**) were characterized using standard analytical and spectroscopic techniques. Thermal gravimetric analysis (TGA) was carried out under a nitrogen atmosphere to study the thermal stability of the complexes. The TGA study was performed in the presence of a nitrogen

https://doi.org/10.1021/acsomega.1c05673
ACS Omega 2022, 7, 1090−1099

gas flow rate of 20 mL/min and a heating rate of 10 °C/min from 30 to 800 °C. All of the TGA data have been included in the Supporting Information (Figures S1−S5).

In the IR spectra of **1**−**5**, distinct bands due to the azomethine (C═N) group are observed at 1591, 1596, 1614.49, 1594, 1627.55 cm^{-1}, whereas the same bands appear at 1630.00, 1630.82, 1629.89, and 1632.60 cm^{-1} for free ligands **L1**−**L4** (Table S4). The shift of these bands toward higher and lower frequencies on complexation with the metal suggests coordination via the imino nitrogen atom in all of the complexes.[21] The C−O phenolic mode is present as a very strong band at about 1211−1272 cm^{-1}. The peaks in the range of 1065−1066 cm^{-1} are assigned to alcoholic C−O stretches. Several weak peaks observed for complexes in the range of 3058−2859 cm^{-1} are ascribed to the aliphatic and aromatic C−H stretches, and the range of 717−744 cm^{-1} is attributed to the C−H out-of-plane bending mode. Broad peaks are observed in the range of 3205−3386 cm^{-1} due to the presence of alcoholic OH groups. Sharp, strong, single peaks are observed at 1058.74 and 1054.61 cm^{-1} for the perchlorate ion present in complexes **3** and **5**, respectively. The broad band at around 3483 cm^{-1} in compound **3** is assigned to the OH stretching vibration of the coordinated water molecules, which are involved in hydrogen bonding.[22]

The electronic spectra for **1**−**5** were recorded in DMSO solvent in the range of 265−700 nm at room temperature using the same solvent as that for the blank. The absorption maxima were observed at 355, 353, 279 and 377, 355, and 280 and 379 nm, respectively, for **1**−**5** (Figure 1). **1**, **2**, and **4** show

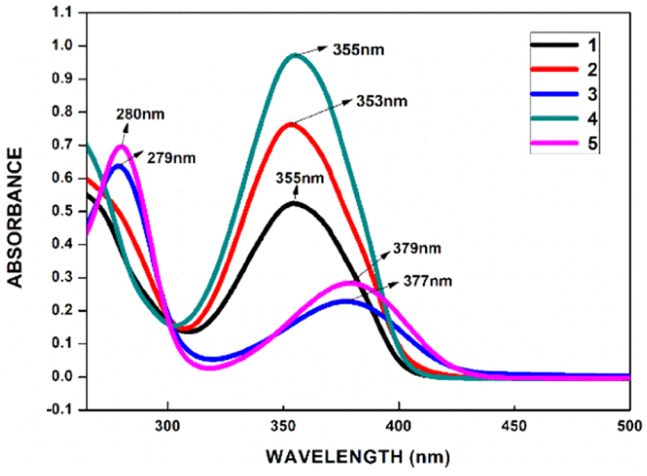

Figure 1. UV−vis spectra of **1**−**5** in solution state in DMSO at room temperature.

a similar kind of absorption maxima where DBM is present, and **3** and **5** show a similar kind of absorption maxima where DBM is absent and only Schiff base is present (Figures S13 and S15). This indicates the similar solution behavior of the compounds. The electronic transition for **1**, **2**, and **4** might be due to the intraligand charge transfer (ILCT).[23] Similarly, the electronic transition for compounds **3** and **5**, the two observed bands, may arise from $\pi \rightarrow \pi^*$ ILCT.

To understand in detail the electronic transition behavior of **1**, **2**, and **4**, DFT calculations[24] for **1** were performed. DFT calculations show that the transition corresponding to 352.79 nm is for the H-2 → L/H-3 → L/H-4 → L/H-1 → L/H-6 → L molecular orbital (MO) transition of an oscillator strength (f) of 0.0116, which is close to the experimental value of 355 nm (Table S5). The electron clouds of H-1, H-2, H-3, H-4, and H-6 MOs are mainly located on the ligand moiety (Figure 2), and LUMO (L) (Figure 2) is also redistributed throughout the ligand moiety, avoiding the metal atom Zn(II). These imply the possibility of the intraligand charge transfer (ILCT) phenomenon. **3** was taken as a case study for **3**, **5**, and DFT calculations were performed. Analysis shows that the transitions corresponding to 276.77 and 384.22 nm are for the significant contributing orbital H-5 → L+1/H-8 → L+1/H-11 → L and H-1 → L/H-1 → L+1/H → L/H → L+1 transitions of oscillator strength (f) of 0.0169 and 0.0055, respectively, are close to the experimental values of 279 and 377 nm (Table S5). The electronic clouds of the MO mostly lie on the ligand orbitals (Figure S17), which suggests that the transitions correspond to the $\pi \rightarrow \pi^*$ ILCT.

The fluorescence spectra of **1**−**5** (Figure 3) were obtained in DMSO solvent in the region of 350−700 nm by exciting at 375 nm, which implies that **1**, **2**, and **4** have similar kinds of emission spectra, and on the other hand, **3** and **5** are similar. **1**−**5** exhibit only one emission peak at 447, 440, 481, 444, and 483 nm, respectively. In the cases of **1**, **2**, and **4**, emission spectra are 19, 21, and 7 nm blue-shifted blue emission, and for compounds **3** and **5**, emission spectra are 20 and 29 nm red-shifted cyan emission compared to free Schiff-base ligands (Figures S21−S25).

Structure of 1. **1** crystallizes in the orthorhombic $P2_12_12_1$ space group. The molecular structure of 1 (Figure 4) contains one zinc (II) ion and one DBM ligand. The penta-coordinated zinc(II) ion adopts a spherical square pyramid geometry (by SHAPE analysis) (Table S16) with Schiff-base (L1) ligand (O1 N1 O4) and two DBM oxygen (O2 O3) donor groups. Both ligands are attached to zinc(II) in a chelating mode. The Schiff-base ligand is monoprotonated, and the alkyl oxygen atom of the hydroxyl group is not deprotonated (Figure 4). The Zn1−O4 bond distance is 2.496(2) Å, which is longer than the distances found in the literature (Zn−O distance in the literature is 2.419(2) Å).[7a] The four coordination number found in **1** is quite common in the literature for O, N ligated Zn (II) complexes. When the coordination number is increased from four to five, the additional coordination is weak, with Zn (II)···O distances between 2.341(10) and 2.912(12) Å, and the corresponding geometry is highly distorted.[25] The selected bond lengths, bond angles, and packing diagram are given in the Supporting Information (Tables S6 and S7 and Figure S41, respectively).

Structure of 2. **2** crystallizes in the I2/a space group. The asymmetric crystallographic unit contains two zinc(II) ions, an anionic Schiff-base ligand (L2), and two terminally coordinating DBM anions (Figure 5a). The Zn(II)−O complex adopts a cubane core (Figure 7a). The core structure (Figure 5b) is stabilized by two Schiff-base ligands and four DBM molecules. All of the zinc(II) ions in the core are hexacoordinated with slightly distorted octahedral geometry. Zn1 is present in an O_5N-donor environment; among these, the coordination is from three bridging oxygen (O3 O6* O3*) atoms, one nitrogen atom (N1*) from Schiff base, and two terminal oxygen (O1* O2*) atoms from DBM. Another metal ion Zn2 is coordinated with three bridging oxygen (O6 O3* O6*) atoms, one methoxy oxygen (O7) from Schiff base, and two terminal oxygen (O4 O5) atoms from DBM. The Schiff-base ligands bind to the zinc center in a [4.3311] coordination mode, and DBM binds [1.11] based on Harris notation.[26] The

https://doi.org/10.1021/acsomega.1c05673
ACS Omega 2022, 7, 1090−1099

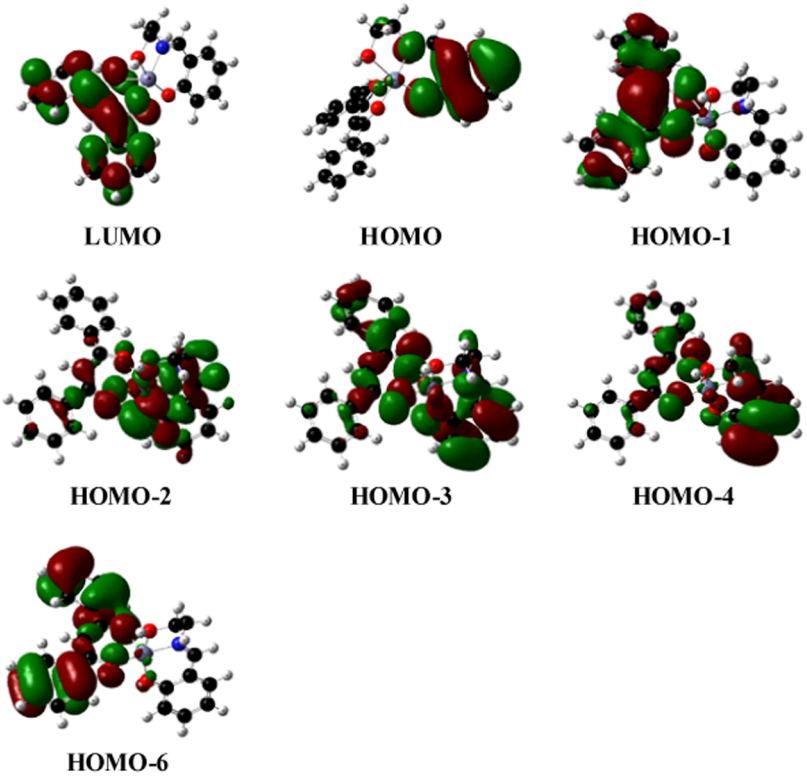

Figure 2. Major contributing molecular orbitals of compound **1** by TD-DFT (time-dependent-density function theory) calculation.

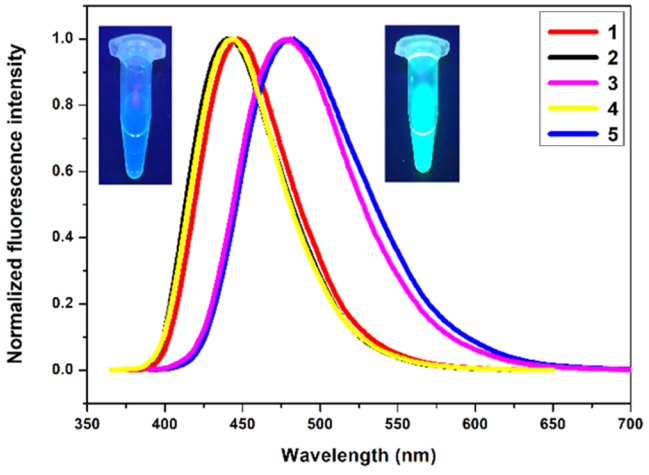

Figure 3. Emission spectra of compounds **1**−**5** in solution state in DMSO solvent at room temperature.

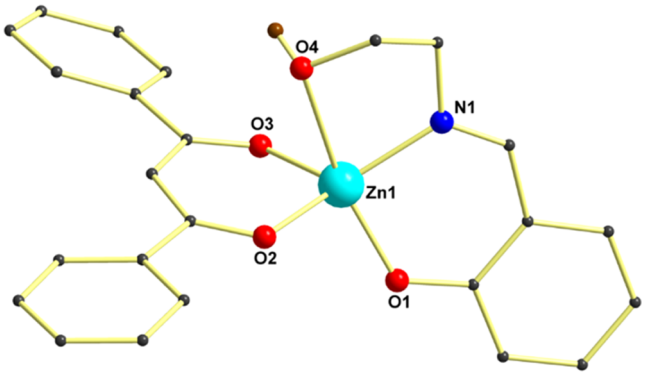

Figure 4. Ball and stick view of the molecular structure of **1**. Hydrogen atoms are removed for clarity. Blue, N; red, O; black, C; brown, H; and cyan, Zn.

selected bond lengths, bond angles, and packing diagram are given in the Supporting Information (Tables S8 and S9 and Figure S42, respectively).

Structure of ***3***. **3** crystallizes in the triclinic P-1 space group. The molecular structure of **3** (Figure 6) contains four Zn(II) ions, four tridentate Schiff-base ligands (L2), and two water molecules that form a distorted cubane core (Figure 7b). In the core, Zn1 is hexacoordinated and present in a distorted octahedral environment with three μ_3-oxo bridging oxygens (O2 O3 O4), one alcoholic oxygen (O1), one nitrogen (N1) from the Schiff-base ligand, and one terminal oxygen (O6) water molecule. Zn3 also has the same hexacoordination distorted octahedrally with three μ_3-oxo bridging oxygens (O2 O4 O5), one alcoholic oxygen (O12), one nitrogen (N3) from the Schiff-base ligand, and terminal oxygen (O11) water molecule. Zn2 is pentacoordinated and present in a distorted square-pyramidal geometry with three μ_3-oxo bridging oxygens (O2 O3 O5), one nitrogen (N2), and one phenolic oxygen (O7). Zn4 hexacoordination is found in a distorted octahedral geometry where zinc atom is surrounded by three μ_3-oxo bridging oxygens (O3 O4 O5), one nitrogen(N4), one phenolic oxygen (O9), and one methoxy (O14) oxygen. Based on Harris notation, the coordination modes found in the Schiff base fall under these three different coordination modes: [3.3111], [3.3110], [3.3110]. The molecule is dicationic, and the charge is balanced by the two perchlorate ions present in the crystal structure, confirmed by the characteristic IR peak at 1058 cm^{-1}. The selected bond lengths, bond angles, and packing diagram are given in the Supporting Information (Tables S10 and S11 and Figure S43, respectively).

https://doi.org/10.1021/acsomega.1c05673
ACS Omega 2022, 7, 1090−1099

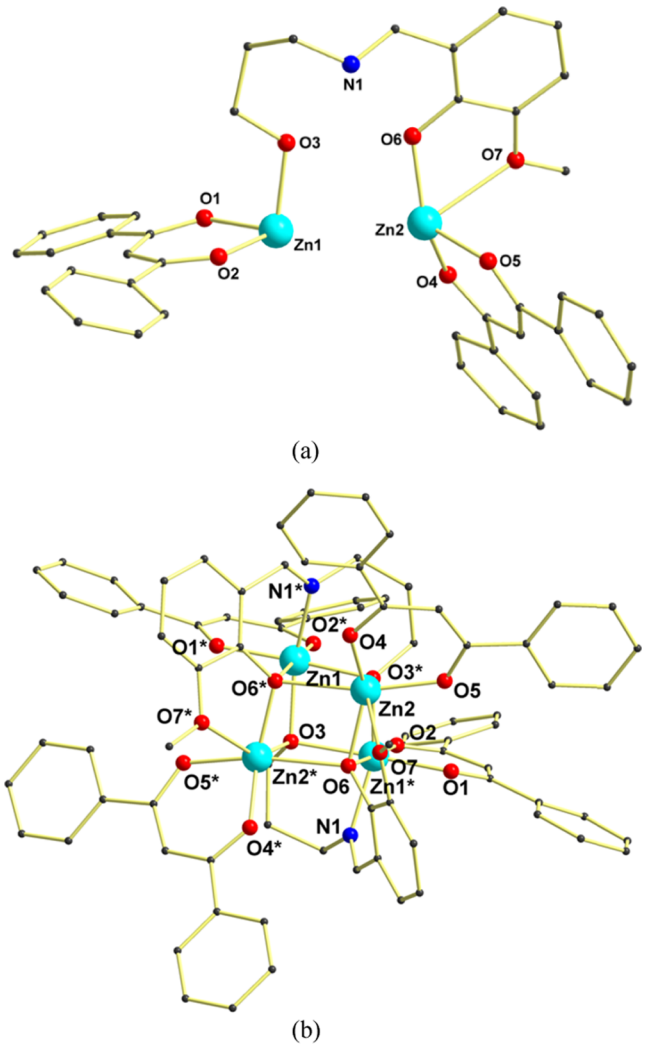

Figure 5. (a) Asymmetric unit of **2** and (b) ball and stick view of the molecular structure of **2**. Hydrogen atoms are removed for clarity. Blue, N; red, O; black, C; and cyan, Zn.

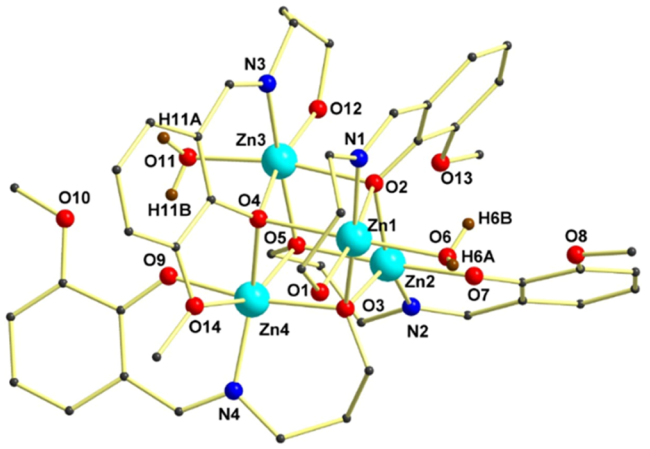

Figure 6. Ball and stick view of the molecular structure of **3**. Hydrogen atoms and counter anions are removed for clarity. Blue, N; red, O; black, C; brown, H; and cyan, Zn.

Structure of ***4***. **4** crystallizes in the triclinic P-1 space group. The molecular structure of **4** (Figure 8a) contains four Zn(II) ions, two Schiff-base ligands (L3), and four DBM molecules in a distorted cubane core. Zn2 and Zn3 are pentacoordinated with three μ_3-oxo bridging oxygens (O4 O7 O8) and (O3 O4 O8) and two DBM oxygens (O5 O6) and (O11 O12), respectively, in a distorted square-pyramidal geometry. Zn1 and Zn4 are hexacoordinated with three μ_3-oxo bridging oxygens (O3 O4 O7) and (O3 O7 O8), one nitrogen (N1 and N2), and two DBM oxygens (O1 O2) and (O9 O10), respectively, and present in a distorted octahedral geometry. In the crystal structure, the two Schiff bases are present in a [4.331] binding mode. In the IR spectrum, the characteristic Schiff-base azomethine peak of compound 4 appears at 1645 and 1594 cm^{-1}. The bond angles, bond lengths, and packing diagram are given in the Supporting Information (Tables S12 and S13 and Figure S44, respectively).

Structure of ***5***. **5** crystallizes in the monoclinic P 2_1/c space group. The asymmetric crystallographic unit contains two zinc (II) ions, two dianionic Schiff-base ligands (L4), and one ethanolamine molecule (Figure 9a). The Zn(II)−O complex adopts a ladderlike core (Figure 9c). In the ladderlike core, Zn1 is present in a six-coordinated distorted octahedral geometry with one μ_3-oxo bridging oxygen (O6), one μ_2-oxo bridging oxygen (O4), one phenolic oxygen (O1), one methoxy oxygen (O2), and one nitrogen (N1). Zn2 is pentacoordinated and found in a distorted square-pyramidal geometry with two μ_3-oxo bridging oxygens (O6 O6*), one μ_2-oxo bridging oxygen (O4), and two nitrogens (N2, N3) as the binding sites. The binding modes of the Schiff base present are in a [1.1110] and [2.2110] fashion. The two bridging ethanolamine moieties stabilize the ladderlike core with a [3.31] binding mode. The whole moiety is dicationic in charge, balanced by the presence of two perchlorate ions characterized crystallographically and from the IR characteristic peak at 1054 cm^{-1}. The peak in the 3386−3310 cm^{-1} range corresponds to two primary amines, and that at 3517 cm^{-1} to the unprotonated alcoholic peak of the Schiff-base ligand. Distinct azomethine peaks appear at 1627 and 1599 cm^{-1}. The bond lengths, bond angles, and packing diagram are given in the Supporting Information (Tables S14 and S15 and Figure S45, respectively).

To summarize, using different methylene chain lengths and in situ generated modified Schiff-base ligands with or without co-ligands, mononuclear zinc Schiff-base complex, cubane, and ladderlike core structures were synthesized and characterized using single-crystal X-ray diffraction.

In zinc-based cluster chemistry, ligand-designed variation in nuclearity and shape of the clusters obtained has not been reported in the literature to date. Herein, by gradually varying the chain lengths of the modified Schiff base used, we have synthesized and structurally characterized clusters of varying sizes and geometry. Though co-ligands have been employed in (**1**, **2**, **4**, and **5**) some cases, they have been found to bind to a single metal ion to saturate its coordination sphere, except for **5**, where excess MEA anion stabilizes the tetranuclear core. Therefore, by varying the chain length of the Schiff bases and using co-ligands, we have added synthetically interesting molecular clusters exhibiting cube and ladder-shaped architecture to the literature.

CONCLUSIONS

Using varying chain lengths containing Schiff-base ligands and auxiliary ligands, mononuclear Zn to tetranuclear Zn_4 cubane complexes, a Zn_4 ladderlike core has been synthesized and characterized. The UV absorption and fluorescence properties

https://doi.org/10.1021/acsomega.1c05673
ACS Omega 2022, 7, 1090−1099

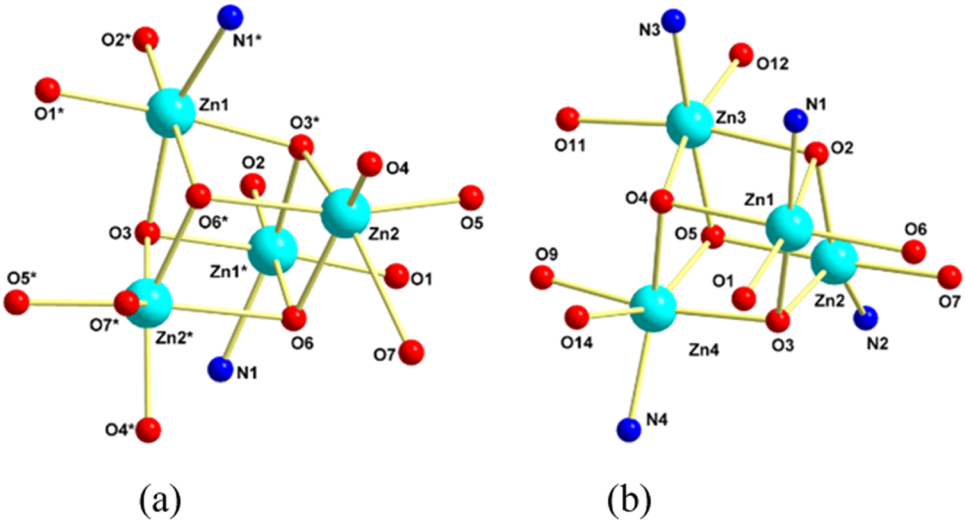

Figure 7. (a) Ball and stick view of the cubane core of **2** and (b) ball and stick view of the cubane core of **3**. Hydrogen atoms are removed for clarity. Blue, N; red, O; black, C; and cyan, Zn.

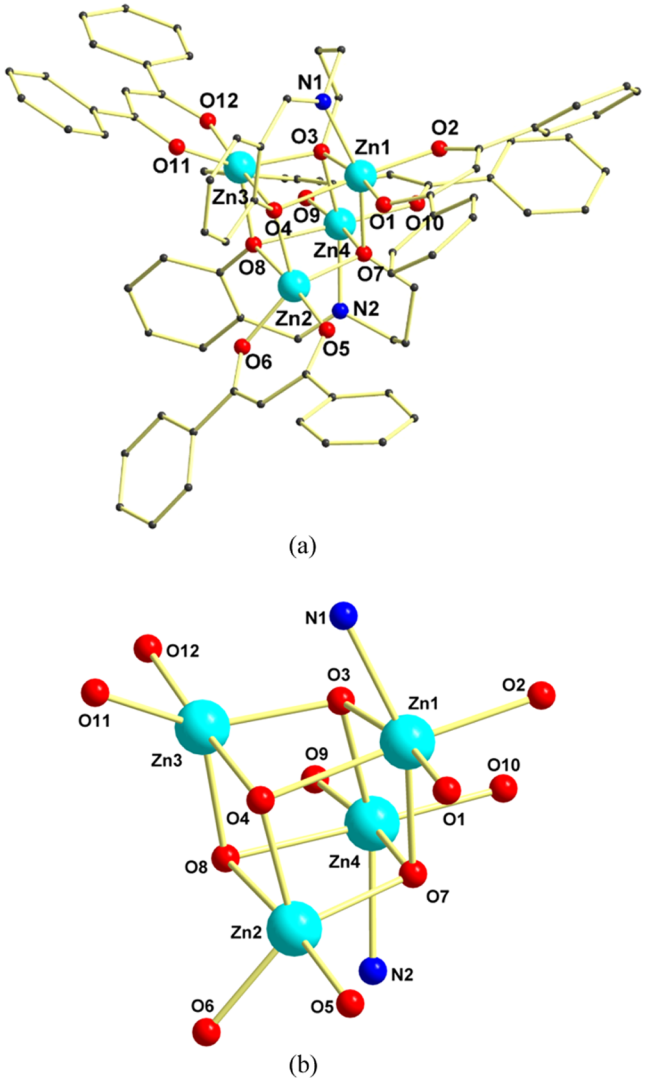

Figure 8. (a) Ball and stick view of the molecular structure of **4**. (b) Cubane core of **4**. Hydrogen atoms are removed for clarity. Blue, N; red, O; black, C; and cyan, Zn.

of the DBM and non-DBM-containing Schiff-base complexes reveal that the UV-absorbing property of DBM is responsible for the blue-shifted absorption maxima compared to the Schiff base containing complex that does not contain DBM. DFT study (for **1**) shows that the LUMO mostly lies on the UV-absorbing DBM moiety, and in the case of **3**, LUMO is redistributed upon the Schiff-base ligands. The absorption maxima of the absorption spectra correspond to the $\pi \rightarrow \pi^*$ ILCT transition.

EXPERIMENTAL SECTION

Instrumentation. Infrared spectra were recorded using a Nicolet iS5 FTIR spectrometer. Elemental analysis was performed using a Flash EA Series 1112 CHNS analyzer. TGA was recorded using a PerkinElmer STA 8000 thermogravimetric analyzer under a nitrogen gas flow rate of 20 mL/min and a heating rate of 10 °C/min. UV−visible spectra were recorded using a Jasco V-750 spectrophotometer, and emission spectra were obtained using a Jasco FP-8500 spectrofluorometer. Single-crystal X-ray data for **1**, **4**, and **5** were collected at 298, 100, 299 K using a Bruker APEX-II CCD diffractometer system [λ (Mo Kα) = 0.71073Å] with a graphite monochromator. The data were reduced using APEX-2, the structures were solved using SHELXS-97 and Olex2, and the data were refined using the program SHELXL-2018/3.[27] The SCXRD data for **2** and **3** were collected at 104 and 100 K with an XtaLAB Synergy, Single source at offset/far, HyPix3000 diffractometer and a Rigaku Oxford HyPix3000 CCD plate detector system [λ (Mo Kα) = 0.71073Å] with a mirror monochromator. Using Olex2,[28] the structure was solved with the ShelXT[29] structure solution program using Intrinsic Phasing and refined with the SHELXL-2018/3[27] refinement package using least-squares minimization. All nonhydrogen atoms were refined anisotropically, and hydrogen atoms were fixed at calculated positions and refined as a riding model. Graphics of the crystal structures have been performed with Diamond (version 2.1e) and Mercury (version 3.10.3) software. In the crystal structures of **2**, **3**, and **4** solvent molecules, voids are present. The present solvent molecules are not structurally determined except in **3** (two dichloromethane molecules). Therefore, for **2** and **4**, electron densities

https://doi.org/10.1021/acsomega.1c05673
ACS Omega 2022, 7, 1090−1099

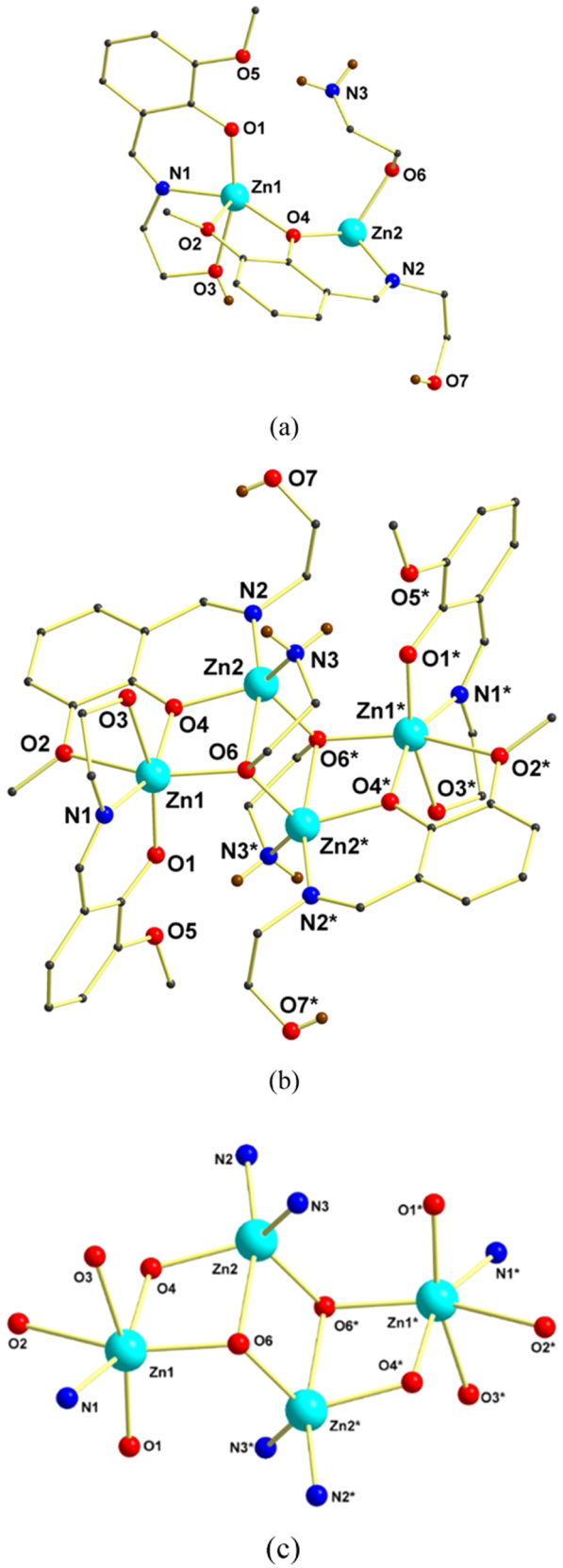

Figure 9. (a) Ball and stick view of the asymmetric unit of **5**. (b) Ball and stick view of **5**. (c) Cubane core of **5**. Hydrogen atoms and counter anions are removed for clarity. Blue, N; red, O; black, C; brown, H; and cyan, Zn.

containing voids were masked out using the Olex2 solvent mask (similar to PLATON/SQUEEZE). The voids for **2** and **4** correspond to $1CHCl_3$ and $1.5CH_2Cl_2$, $0.5H_2O$, respectively. The details of the solvent masks used are appended to the corresponding CIF Files and Supporting Information.

Theoretical Details. Quantum chemical calculations were performed to investigate the experimental outcomes of the Zn(II)−Schiff base complexes. Optimization of the gas-phase ground-electronic-state molecular structure of these complexes was accomplished using the B3LYP theoretical model without considering any symmetry restriction. For optimization in the solvent phase, we considered the Integral Equation Formalism Polarizable Continuum Model (IEFPCM)[30] of DMSO solvent. All of these calculations were executed at the level of density functional theory using a 6-311G basis set[31] for all kinds of atoms. A time-dependent-density function theory (TD-DFT) simulation was performed in the same solvent phase to obtain an elaborate justification of UV−vis spectra. The Gaussian 09W package[32] was used for these calculations.

Preparation of the Schiff-Base Ligand and Complex. *Chemicals, Solvents, and Starting Materials.* **Caution!** All perchlorates, including raw materials and products, are potentially explosive. These materials should be used during the process in a fume hood and handled with care.

High-purity *o*-vanillin (Sigma-Aldrich), salicylaldehyde (Merck), ethanolamine (Avra), 3-aminopropanol (Avra), dibenzoyl methane (DBM) (Sigma-Aldrich), zinc perchlorate hexahydrate (Sigma-Aldrich), and all other solvents were purchased from commercial sources. All solvents were distilled before use, and chemicals were used without further purification.

General Synthesis. Schiff-base ligands L1, L2, L3, and L4 were synthesized via in situ condensation[1] into the reaction medium.

Synthesis of Complexes. For **1**, **3**, **4**, and **5**, similar synthesis procedures were followed. Ligands and co-ligands were taken in 30 mL of methanol−acetonitrile solvent mixture (1:1) and metal salt (zinc perchlorate hexahydrate) was added followed by the dropwise addition of triethylamine base and stirred for 6 h, and different crystallization techniques were performed. Only **2** was stirred for 24 h.

For **1**, salicylaldehyde (0.082 g, 0.770 mmol), monoethanolamine (0.082 mL, 0.770 mmol), DBM (0.172 g, 0.770 mmol), zinc perchlorate (0.286 g, 0.770 mmol), and triethylamine (0.321 mL, 2.31 mmol) were required. After 6 h of a room-temperature reaction, the yellowish solution was filtered and the volume was reduced to 10 mL. Yellowish crystals were obtained overnight and collected and analyzed. Yield: 0.310 g, 89.15% (based on $Zn(ClO_4)_2$, $6H_2O$). Anal. calcd. (%) for $C_{24}H_{21}NO_4Zn$(452.83): C, 63.66; H, 4.67; N, 3.09. Found: C, 63.63; H, 4.71; N, 3.12. ^{1}H NMR (500 MHz, DMSO-d_6): δ = 8.39 (s, 1H, CH═N), 8.04−8.06 (m, 4H, Ar H), 7.47−7.54 (m, 6H, Ar H), 7.15−7.25 (m, 2H, Ar H), 6.78 (s, 1H, CH), 6.59−6.61 (d, 1H, Ar H), 6.43−6.54 (m, 1H, Ar H), 5.07 (br,1H, CH_2OH), 3.57−3.72 (m, 4H,) ^{13}C NMR (125 MHz, DMSO-d_6): δ = 185.96, 172.54, 170.59, 140.65, 136.48, 134.64, 131.46, 128.82, 127.62, 122.76, 118.79, 113.97, 92.79, 62.43, 60.43 (selected IR bands: $\tilde{\nu}$ (cm^{-1}) = 3205, 1591, 1519, 1233, 1065, 744).

For **2**, *o*-vanillin (0.117 g, 0.770 mmol), 3-aminopropanol (0.058 mL, 0.770 mmol), DBM (0.172 g, 0.770 mmol), zinc perchlorate (0.286 g, 0.770 mmol), and triethylamine (0.321 mL, 2.31 mmol) were required. Within 30 min, a white

https://doi.org/10.1021/acsomega.1c05673
ACS Omega 2022, 7, 1090−1099

precipitate began to be thrown out from the reaction medium. Stirring was continued for 24 h for complete precipitation. The precipitate was filtered and crystallized in chloroform/hexane using the diffusion method. X-ray quality crystals were obtained in a week's time. Yield: 0.240 g, 74.05% (based on $Zn(ClO_4)_2$, $6H_2O$). Anal. calcd. (%) for $C_{83}H_{71}Cl_3N_2O_{14}Zn_4$ (1688.24): C, 59.05; H, 4.24; N, 1.66. Found: C, 59.09; H, 4.32; N, 1.68. ^{1}H NMR (500 MHz, DMSO-d_6): δ = 8.23 (s, 2H, CH═N), 8.05−8.06 (m, Ar H), 7.47−7.54 (m, 24H, Ar H), 6.78 (s, 4H, C═CH), 6.75−6.81 (d, 4H, Ar H), 6.36−6.39 (t, 2H, Ar H), 3.83−4.33 (m, 8H, CH_2O CH_2N), 3.69 (s, 6H, OMe), 1.83 (m, 4H, CH_2) ^{13}C NMR (125 MHz, DMSO-d_6): δ = 186.03, 172.56, 140.68, 131.43, 128.79, 127.60, 92.79, 56.12 (selected IR bands: $\tilde{\nu}$ (cm^{-1}) = 1596, 1452, 1222, 1066, 717).

For **3**, *o*-vanillin (0.117 g, 0.770 mmol), 3-aminopropanol (0.058 mL, 0.770 mmol), zinc perchlorate (0.286 g, 0.770 mmol), and triethylamine (0.321 mL, 2.31 mmol) were required. Stirring was continued for 6 h for completion of the reaction. The solvent was evaporated with rotor-vapor and crystallized in a DCM/hexane mixture using the diffusion method. X-ray quality crystals were obtained in 2 weeks. Yield: 0.190 g, 66.10% (based on $Zn(ClO_4)_2$, $6H_2O$). Anal. calcd. (%) for $C_{46}H_{62}Cl_6N_4O_{22}Zn_4$ (1497.17): C, 36.90; H, 4.17; N, 3.74. Found: C, 36.82; H, 4.21; N, 3.70. ^{1}H NMR (500 MHz, DMSO-d_6): δ = 8.24 (s, 4H, CH═N), 6.75−6.86 (m, 8H, Ar H), 6.37−6.43 (m, 4H, Ar H), 3.69 (s, 12H, OMe), 3.46−3.61 (m, 16H, NCH_2 and OCH_2), 1.78 (m, 8H, CH_2) ^{13}C NMR (125 MHz, DMSO-d_6): δ = 168.60, 161.39, 152.56, 152.28, 127.55, 126.71, 118.31, 118.11, 113.74, 112.22, 69.14, 62.73, 55.98, 55.72, 55.38, 36.39, 33.21 (selected IR bands: $\tilde{\nu}$ (cm^{-1}) = 3483, 1614, 1442, 1211, 1058, 733, 1058).

For **4**, salicylaldehyde (0.082 g, 0.770 mmol), 3-aminopropanol (0.058 mL, 0.770 mmol), DBM (0.172 g, 0.770 mmol), zinc perchlorate (0.286 g, 0.770 mmol), and triethylamine (0.321 mL, 2.31 mmol) were required. After 6 h of stirring, the reaction mixture was filtered, evaporated with rotor-vapor, and crystallized in a DCM/hexane layer method at 0 °C. X-ray quality crystals were obtained within 2 weeks. Yield: 0.200 g, 66.33% (based on $Zn(ClO_4)_2$, $6H_2O$). Anal. calcd. (%) for $C_{81.50}H_{70}Cl_3N_2O_{12.50}Zn_4$ (1645.22): C, 59.50; H, 4.29; N, 1.70. Found: C, 59.61; H, 4.53; N, 1.68.^{1}H NMR (500 MHz, DMSO-d_6): δ = 8.24 (s, 2H, CH═N), 8.04−8.05 (m, 16H, Ar H), 7.46−7.53 (m, 24H, Ar H), 7.13−7.17 (m,4H, Ar H), 6.78 (s, 4H, C−H), 6.57−6.61 (m, 2H, Ar H), 6.45−6.48 (m, 2H, Ar H), 3.61−3.74 (m, 4H, CH_2N), 3.36−3.44 (m, 4H, CH_2O), 1.67−1.69 (m, 4H, CH_2), ^{13}C NMR (125 MHz, DMSO-d_6): δ = 186.03, 172.56, 170.73, 140.67, 136.57, 135.95, 134.88, 133.76, 131.44, 128.80, 127.60, 122.70, 114.29, 113.02, 92.80, 59.09, 58.07, 57.53, 55.35, 34.66, 33.90, (selected IR bands: $\tilde{\nu}$ (cm^{-1}) = 1594, 1474, 1272, 1065, 716).

For **5**, *o*-vanillin (0.117 g, 0.770 mmol), ethanolamine (0.069 mL, 1.155 mmol), zinc perchlorate (0.286 g, 0.770 mmol), and triethylamine (0.321 mL, 2.31 mmol) were required. Stirring was continued for 6 h. The clear solution was filtered and evaporated. The oily residue was dissolved in DCM and crystallized in a DCM/hexane layer method at 0 °C. X-ray quality crystals were obtained within 1 week. Yield: 0.210 g, 80.58% (based on $Zn(ClO_4)_2$, $6H_2O$). Anal. calcd. (%) for $C_{44}H_{60}Cl_2N_6O_{22}Zn_4$ (1357.36): C, 38.93; H, 4.46; N, 6.19. Found: C, 38.87; H, 4.53; N, 6.23. ^{1}H NMR (500 MHz, DMSO-d_6): δ = 8.57(s, 2H, CH═N), 8.37 (s, 2H, CH═N), 6.84−6.87 (m, 8H, Ar H), 6.42−6.46 (m, 4H, Ar H), 5.64 (br, 4H, NH_2), 3.68 (s, 12H, OMe), 3.62 (m, 8H, CH_2N), 3.50 (m, 8H, CH_2O), 2.74 (m, 4H, CH_2N), 2.51−2.55 (m, 4H, CH_2O), ^{13}C NMR (125 MHz, DMSO-d_6): δ = 172.48, 171.39, 164.80, 162.95, 161.76, 127.92, 127.63, 118.18, 118.00, 115.49, 114.94, 113.58, 112.86, 112.64, 64.35, 62.25, 60.44, 60.13, 59.70, 58.63, 56.57, 56.07, 55.95, 55.38, 49.07, 44.99, 42.81 (selected IR bands: $\tilde{\nu}$ (cm^{-1}) = 3538, 1627, 1449, 1212, 1054, 740).

■ ASSOCIATED CONTENT

Supporting Information

The Supporting Information is available free of charge at https://pubs.acs.org/doi/10.1021/acsomega.1c05673.

UV−vis spectrum; emission spectrum; IR; TGA; PXRD; ^{1}H; ^{13}C NMR; TD-DFT calculations; and shape calculations (PDF)

Crystallographic data (CIF)

Accession Codes

CCDC 2102608−2102612 contain the supplementary crystallographic data for this paper. These data can be obtained free of charge via www.ccdc.cam.ac.uk/data_request/cif, or by emailing data_request@ccdc.cam.ac.uk, or by contacting The Cambridge Crystallographic Data Centre, 12 Union Road, Cambridge CB2 1EZ, UK; fax: +44 1223 336033.

■ AUTHOR INFORMATION

Corresponding Author

Viswanathan Baskar − *School of Chemistry, University of Hyderabad, Hyderabad 500046 Telangana, India;* orcid.org/0000-0002-5270-3272; Phone: +91-40-23134825; Email: vbsc@uohyd.ac.in

Authors

Suman Mondal − *School of Chemistry, University of Hyderabad, Hyderabad 500046 Telangana, India*

Smruti Prangya Behera − *School of Chemistry, University of Hyderabad, Hyderabad 500046 Telangana, India*

Mohammed Alamgir − *School of Chemistry, University of Hyderabad, Hyderabad 500046 Telangana, India*

Complete contact information is available at: https://pubs.acs.org/10.1021/acsomega.1c05673

Notes

The authors declare no competing financial interest.

■ ACKNOWLEDGMENTS

V.B. thanks UPE-II for funding. S.M. and S.P.B. thank UGC for a fellowship. M.A. thanks CSIR for a fellowship.

■ REFERENCES

(1) (a) Murugavel, R.; Kuppuswamy, S.; Boomishankar, R.; Steiner, A. Hierarchical structures built from a molecular zinc phosphate core. *Angew. Chem., Int. Ed.* **2006**, *45*, 5536−5540. (b) Dar, A. A.; Sen, S.; Gupta, S. K.; Patwari, G. N.; Murugavel, R. Octanuclear zinc phosphates with hitherto unknown cluster architectures: ancillary ligand and solvent assisted structural transformations thereof. *Inorg. Chem.* **2015**, *54*, 9458−9469. (c) Bar, A. K.; Kalita, P.; Sutter, J. P.; Chandrasekhar, V. Pentagonal-bipyramid Ln (III) complexes exhibiting single-ion-magnet behavior: a rational synthetic approach for a rigid equatorial plane. *Inorg. Chem.* **2018**, *57*, 2398−2401. (d) Yadav, M.; Mondal, A.; Mereacre, V.; Jana, S. K.; Powell, A. K.; Roesky, P. W. Tetranuclear and pentanuclear compounds of the rare-earth metals: synthesis and magnetism. *Inorg. Chem.* **2015**, *54*, 7846−

7856. (e) Li, L.; Gou, J.; Wu, D. F.; Wang, Y. J.; Duan, Y. Y.; Chen, H. H.; Gao, H. L.; Cui, J. Z. Near-infrared luminescence and magnetic properties of dinuclear rare earth complexes modulated by β-diketone co-ligands. *New J. Chem.* **2020**, *44*, 3912−3921.
(2) (a) Baskar, V.; Shanmugam, M.; Sañudo, E. C.; Shanmugam, M.; Collison, D.; McInnes, E. J.; Wei, Q.; Winpenny, R. E. Metal cages using a bulky phosphonate as a ligand. *Chem. Commun.* **2007**, 37−39. (b) Ali, S.; Baskar, V.; Muryn, C. A.; Winpenny, R. E. Mixed antimonate-phosphonate ligands as polydentate bridging oxygen donors. *Chem. Commun.* **2008**, *47*, 6375−6377.
(3) Chandrasekhar, V.; Nagarajan, L.; Gopal, K.; Baskar, V.; Kögerler, P. A new structural form for a decanuclear copper (II) assembly. *Dalton Trans.* **2005**, *148*, 3143−3145.
(4) Baskar, V.; Gopal, K.; Helliwell, M.; Tuna, F.; Wernsdorfer, W.; Winpenny, R. E. 3d−4f Clusters with large spin ground states and SMM behaviour. *Dalton Trans.* **2010**, *39*, 4747−4750.
(5) Ali, J.; Navaneetha, T.; Baskar, V. Bismuth and Titanium Phosphinates: Isolation of Tetra-, Hexa-and Octanuclear Clusters. *Inorg. Chem.* **2020**, *59*, 741−747.
(6) Ugandhar, U.; Navaneetha, T.; Ali, J.; Mondal, S.; Vaitheeswaran, G.; Baskar, V. Assembling Homometallic Sb_6 and Heterometallic Ti_4Sb_2 Oxo Clusters. *Inorg. Chem.* **2020**, *59*, 6689−6696.
(7) (a) Dey, M.; Rao, C. P.; Saarenketo, P.; Rissanen, K.; Kolehmainen, E. Four-, Five-and Six-Coordinated ZnII Complexes of OH-Containing Ligands: Syntheses, Structure and Reactivity. *Eur. J. Inorg. Chem.* **2002**, *8*, 2207−2215. (b) Akine, S.; Dong, W.; Nabeshima, T. Octanuclear zinc (II) and cobalt (II) clusters produced by cooperative tetrameric assembling of oxime chelate ligands. *Inorg. Chem.* **2006**, *45*, 4677−4684. (c) Nihei, M.; Yoshida, A.; Koizumi, S.; Oshio, H. Hetero-metal Mn−Cu and Mn−Ni clusters with tridentate Schiff-base ligands. *Polyhedron* **2007**, *26*, 1997−2007. (d) Gao, Q.; Qin, Y.; Chen, Y.; Liu, W.; Li, H.; Wu, B.; Li, Y.; Li, W. Cubane-type $\{M_4O_4\}$ (M = Co II, Zn II, Cu II) clusters: synthesis, crystal structures, and luminescent and magnetic properties. *RSC Adv.* **2015**, *5*, 43195−43201. (e) Kushvaha, S. K.; Arumugam, S.; Shankar, B.; Sarkar, R. S.; Ramkumar, V.; Mondal, K. C. Isolation and Characterization of Different Homometallic and Heterobimetallic Complexes of Nickel and Zinc Ions by Controlling Molar Ratios and Solvents. *Eur. J. Inorg. Chem.* **2019**, *2019*, 2871−2882.
(8) (a) Xiang, H.; Lan, Y.; Jiang, L.; Zhang, W. X.; Anson, C. E.; Lu, T. B.; Powell, A. K. A chiral tetranuclear copper (II) complex based on a new Schiff-base ligand: Synthesis, structure, magnetic property and CD spectra. *Inorg. Chem. Commun.* **2012**, *16*, 51−54. (b) Ahamad, M. N.; Iman, K.; Raza, M. K.; Kumar, M.; Ansari, A.; Ahmad, M.; Shahid, M. Anticancer properties, apoptosis and catecholase mimic activities of dinuclear cobalt (II) and copper (II) Schiff base complexes. *Bioorg. Chem.* **2020**, *95*, No. 103561. (c) Constable, E. C.; Housecroft, C. E.; Zampese, J. A.; Zhang, G. Multinuclear zinc (II) complexes with $\{Zn_6\ (\mu\text{-O})_6\ (\mu 3\text{-O})_2\}$-and $\{Zn_5\ (\mu\text{-O})_3\ (\mu 3\text{-O})_3\}$-cluster cores. *Polyhedron* **2012**, *44*, 150−155. (d) Liu, Z. Y.; Zou, H. H.; Wang, R.; Chen, M. S.; Liang, F. P. Structure and magnetism of two chair-shaped hexanuclear dysprosium (III) complexes exhibiting slow magnetic relaxation. *RSC Adv.* **2018**, *8*, 767−774. (e) Shit, S.; Nandy, M.; Rosair, G.; El Fallah, M. S.; Ribas, J.; Garribba, E.; Mitra, S. A hexanuclear copper (II) Schiff base complex incorporating rare "bicapped cubane" core: Structural aspects, magnetic properties and EPR study. *Polyhedron* **2013**, *52*, 963−969. (f) Tsantis, S. T.; Tzimopoulos, D. I.; Holynska, M.; Perlepes, S. P. Oligonuclear Actinoid Complexes with Schiff Bases as Ligands—Older Achievements and Recent Progress. *Int. J. Mol. Sci.* **2020**, *21*, No. 555. (g) Biswas, R.; Drew, M. G.; Ghosh, A. Synthesis and crystal structure of a novel octa-aqua bridged star-shaped Ni_4K complex. *Inorg. Chem. Commun.* **2012**, *24*, 1−3. (h) Griffiths, K.; Kühne, I. A.; Tizzard, G. J.; Coles, S. J.; Kostakis, G. E.; Powell, A. K. Twists to the spin structure of the Ln_9-diabolo motif exemplified in two $\{Zn_2Ln_2\}$ $[Ln_9]$ $\{Zn_2\}$ coordination clusters. *Inorg. Chem.* **2019**, *58*, 2483−2490. (i) Georgopoulou, A. N.; Pissas, M.; Psycharis, V.; Sanakis, Y.; Raptopoulou, C. P. Trinuclear NiII-LnIII-NiII Complexes with Schiff Base Ligands: Synthesis, Structure, and Magnetic Properties. *Molecules* **2020**, *25*, No. 2280.
(9) (a) Lin, P. H.; Burchell, T. J.; Ungur, L.; Chibotaru, L. F.; Wernsdorfer, W.; Murugesu, M. A polynuclear lanthanide single-molecule magnet with a record anisotropic barrier. *Angew. Chem.* **2009**, *121*, 9653−9656. (b) Sun, W. B.; Han, B. L.; Lin, P. H.; Li, H. F.; Chen, P.; Tian, Y. M.; Murugesu, M.; Yan, P. F. Series of dinuclear and tetranuclear lanthanide clusters encapsulated by salen-type and β-diketionate ligands: single-molecule magnet and fluorescence properties. *Dalton Trans.* **2013**, *42*, 13397−13403.
(10) (a) Gao, B.; Duan, R.; Pang, X.; Li, X.; Qu, Z.; Shao, H.; Wang, X.; Chen, X. Zinc complexes containing asymmetrical N, N, O-tridentate ligands and their application in lactide polymerization. *Dalton Trans.* **2013**, *42*, 16334−16342. (b) Duan, R.; Gao, B.; Li, X.; Pang, X.; Wang, X.; Shao, H.; Chen, X. Zinc complexes bearing tridentate O, N, O-type half-Salen ligands for ring-opening polymerization of lactide. *Polymer* **2015**, *71*, 1−7. (c) Virachotikul, A.; Laiwattanapaisarn, N.; Wongmahasirikun, P.; Piromjitpong, P.; Chainok, K.; Phomphrai, K. Ring-Opening Copolymerizaton of Cyclohexene Oxide and Succinic Anhydride by Zinc and Magnesium Schiff-Base Complexes Containing Alkoxy Side Arms. *Inorg. Chem.* **2020**, *59*, 8983−8994. (d) Ghosh, S.; Spannenberg, A.; Mejía, E. Cubane-Type Polynuclear Zinc Complexes Containing Tridentate Schiff Base Ligands: Synthesis, Characterization, and Ring-Opening Polymerization Studies of rac-Lactide and ε-Caprolactone. *Helv. Chim. Acta* **2017**, *100*, No. e1700176.
(11) Bernardo, K.; Leppard, S.; Robert, A.; Commenges, G.; Dahan, F.; Meunier, B. Synthesis and characterization of new chiral Schiff base complexes with diiminobinaphthyl or diiminocyclohexyl moieties as potential enantioselective epoxidation catalysts. *Inorg. Chem.* **1996**, *35*, 387−396.
(12) (a) Chisholm, M. H.; Gallucci, J. C.; Zhen, H.; Huffman, J. C. Three-coordinate zinc amide and phenoxide complexes supported by a bulky Schiff base ligand. *Inorg. Chem.* **2001**, *40*, 5051−5054. (b) Orabi, A. S.; Abou El-Nour, K. M.; Youssef, M. F.; Salem, H. A. Novel and highly effective composites of silver and zinc oxide nanoparticles with some transition metal complexes against different microorganisms. *Arab. J. Chem.* **2020**, *13*, 2628−2648. (c) Pushpanathan, V.; Kumar, D. S. A novel zinc (II) macrocycle-based synthesis of pure ZnO nanoparticles. *J. Nanostruct. Chem.* **2014**, *4*, 95−101.
(13) (a) Chowdhury, T.; Dasgupta, S.; Khatua, S.; Acharya, K.; Das, D. Executing a Series of Zinc (II) Complexes of Homologous Schiff Base Ligands for a Comparative Analysis on Hydrolytic, Anti-oxidant and Anti-bacterial Activities. *ACS Appl. Bio Mater.* **2020**, *3*, 4348−4357. (b) Tsave, O.; Halevas, E.; Yavropoulou, M. P.; Papadimitriou, A. K.; Yovos, J. G.; Hatzidimitriou, A.; Gabriel, C.; Psycharis, V.; Salifoglou, A. Structure-specific adipogenic capacity of novel, well-defined ternary Zn (II)-Schiff base materials. Biomolecular correlations in zinc-induced differentiation of 3T3-L1 pre-adipocytes to adipocytes. *J. Inorg. Biochem.* **2015**, *152*, 123−137. (c) Dey, D.; Kaur, G.; Ranjani, A.; Gayathri, L.; Chakraborty, P.; Adhikary, J.; Pasan, J.; Dhanasekaran, D.; Choudhury, A. R.; Akbarsha, M. A.; Kole, N.; et al. A trinuclear zinc−schiff base complex: biocatalytic activity and cytotoxicity. *Eur. J. Inorg. Chem.* **2014**, *2014*, 3350−3358. (d) Das, S.; Sahu, A.; Joshi, M.; Paul, S.; Shit, M.; Choudhury, A. R.; Biswas, B. Ligand-Centered Radical Activity by a Zinc-Schiff-Base Complex towards Catechol Oxidation. *ChemistrySelect* **2018**, *3*, 10774−10781. (e) Garai, M.; Das, A.; Joshi, M.; Paul, S.; Shit, M.; Choudhury, A. R.; Biswas, B. Synthesis and spectroscopic characterization of a photo-stable tetrazinc (II)−Schiff base cluster: A rare case of ligand centric phenoxazinone synthase activity. *Polyhedron* **2018**, *156*, 223−230.
(14) (a) Sun, W.; Qin, X. T.; Zhang, G. N.; Ding, S.; Wang, Y. Q.; Liu, Z. L. Two novel tetranuclear zinc (II) clusters with different topological structures: Crystal structures and luminescence properties. *Inorg. Chem. Commun.* **2014**, *40*, 190−193. (b) Ghosh, T. K.; Jana, S.; Ghosh, A. Exploitation of the Flexidentate Nature of a Ligand to Synthesize Zn (II) Complexes of Diverse Nuclearity and Their Use in Solid-State Naked Eye Detection and Aqueous Phase Sensing of 2, 4,

https://doi.org/10.1021/acsomega.1c05673
ACS Omega 2022, 7, 1090−1099

6-Trinitrophenol. *Inorg. Chem.* **2018**, *57*, 15216−15228. (c) Yu, H.; Liu, M.; Gao, X.; Liu, Z. Construction and crystal structure of a pair of tetranuclear Zn (II) chiral clusters that exhibit ferroelectric behavior under a higher frequency electric field at room temperature. *Polyhedron* **2017**, *137*, 217−221.

(15) (a) Dasgupta, S.; Karim, S.; Banerjee, S.; Saha, M.; Saha, K. D.; Das, D. Designing of novel zinc (II) Schiff base complexes having acyl hydrazone linkage: study of phosphatase and anti-cancer activities. *Dalton Trans.* **2020**, *49*, 1232−1240. (b) Strinoiu, M.; Răducă, M.; Mădălan, A. M. Zinc (II) mononuclear complexes with Schiff base derivatives of 2-aminofluorene. Synthesis, structural characterization, and optical properties. *J. Coord. Chem.* **2020**, *73*, 2786−2800.

(16) Sanatkar, T. H.; Khorshidi, A.; Janczak, J. Dinuclear Zn (II) and tetranuclear Co (II) complexes of a tetradentate N_2O_2 Schiff base ligand: Synthesis, crystal structure, characterization, DFT studies, cytotoxicity evaluation, and catalytic activity toward benzyl alcohol oxidation. *Appl. Organomet. Chem.* **2020**, *34*, No. 5493.

(17) (a) Karmakar, M.; Chattopadhyay, S. Synthesis, structure and nitroaromatic sensing ability of a trinuclear zinc complex with a reduced Schiff base ligand: Assessment of the ability of the ligand to sense zinc ion. *Polyhedron* **2020**, *187*, No. 114639. (b) Fondo, M.; Ocampo, N.; García-Deibe, A. M.; Sanmartín, J. Zn3, Ni3, and Cu3 Complexes of a Novel Tricompartmental Acyclic Ligand. *Inorg. Chem.* **2009**, *48*, 4971−4979.

(18) Yang, C.; Peng, Y.; Wang, J.; Chen, P.; Gong, X. Syntheses, structures and catalysis of tetranuclear zinc N-alkoxide ketoiminate complexes for ring-opening polymerization of rac-lactide. *Inorg. Chem. Commun.* **2020**, *119*, 108136.

(19) (a) Kushvaha, S. K.; Shankar, B.; Gorantla, N. S. M.; Mondal, K. C. A Fluorescent Hexanuclear Zn (II) Complex. *ChemistrySelect* **2019**, *4*, 3334−3339. (b) Roy, P.; Manassero, M.; Dhara, K.; Banerjee, P. Synthesis, characterization and fluorescence properties of hexanuclear zinc (II) complexes. *Polyhedron* **2009**, *28*, 1133−1137. (c) Gheorghe, R.; Ionita, G. A.; Maxim, C.; Caneschi, A.; Sorace, L.; Andruh, M. Aggregation of heptanuclear [MII7] (M= Co, Ni, Zn) clusters by a Schiff-base ligand derived from o-vanillin: Synthesis, crystal structures and magnetic properties. *Polyhedron* **2019**, *171*, 269−278.

(20) (a) Dismukes, G. C. The metal centers of the photosynthetic oxygen-evolving complex. *Photochem. Photobiol.* **1986**, *43*, 99−115. (b) Renger, G. Biological exploitation of solar energy by photosynthetic water splitting. *Angew. Chem., Int. Ed.* **1987**, *26*, 643−660. (c) Lee, H. B.; Marchiori, D. A.; Chatterjee, R.; Oyala, P. H.; Yano, J.; Britt, R. D.; Agapie, T. S= 3 Ground State for a Tetranuclear MnIV4O4 Complex Mimicking the S3 State of the Oxygen-Evolving Complex. *J. Am. Chem. Soc.* **2020**, *142*, 3753−3761. (d) Wang, J.; Meng, X.; Xie, W.; Zhang, X.; Fan, Y.; Wang, M. Two biologically inspired tetranuclear nickel (II) catalysts: effect of the geometry of Ni_4 core on electrocatalytic water oxidation. *J. Biol. Inorg. Chem.* **2021**, *26*, 205−216.

(21) Dolaz, M.; Tümer, M.; Diğrak, M. Synthesis, characterization and stability constants of polynuclear metal complexes. *Transition Met. Chem.* **2004**, *29*, 528−536.

(22) (a) Chattopadhyay, S.; Ray, M. S.; Drew, M. G.; Figuerola, A.; Diaz, C.; Ghosh, A. Facile synthesis of Cu (II) complexes of monocondensed N, N, N donor Schiff base ligands: Crystal structure, spectroscopic and magnetic properties. *Polyhedron* **2006**, *25*, 2241−2253. (b) Sinha Ray, M.; Chattopadhyay, S.; Drew, M. G.; Figuerola, A.; Ribas, J.; Diaz, C.; Ghosh, A. Trinuclear CuII Complexes Containing Peripheral Ketonic Oxygen Bridges and a μ3-OH Core: Syntheses, Crystal Structures, Spectroscopic and Magnetic Properties. *Ber. Dtsch. Chem. Ges.* **2005**, 4562−4571.

(23) (a) Pal, C. K.; Mahato, S.; Joshi, M.; Paul, S.; Choudhury, A. R.; Biswas, B. Transesterification activity by a zinc (II)-schiff base complex with theoretical interpretation. *Inorg. Chim. Acta* **2020**, *506*, No. 119541. (b) Jiang, L.; Zhang, D. Y.; Suo, J. J.; Gu, W.; Tian, J. L.; Liu, X.; Yan, S. P. Synthesis, magnetism and spectral studies of six defective dicubane tetranuclear $\{M_4O_6\}$(M= Ni II, Co II, Zn II) and three trinuclear Cd II complexes with polydentate Schiff base ligands. *Dalton Trans.* **2016**, *45*, 10233−10248. (c) Wang, H.; Zhang, D.; Ni, Z. H.; Li, X.; Tian, L.; Jiang, J. Synthesis, crystal structures, and luminescent properties of phenoxo-bridged heterometallic trinuclear propeller-and sandwich-like Schiff-base complexes. *Inorg. Chem.* **2009**, *48*, 5946−5956.

(24) (a) Vladimirova, K. G.; Freidzon, A. Y.; Kotova, O. V.; Vaschenko, A. A.; Lepnev, L. S.; Bagatur'yants, A. A.; Vitukhnovskiy, A. G.; Stepanov, N. F.; Alfimov, M. V. Theoretical study of structure and electronic absorption spectra of some Schiff bases and their zinc complexes. *Inorg. Chem.* **2009**, *48*, 11123−11130. (b) Sarkar, A.; Chakraborty, A.; Chakraborty, T.; Purkait, S.; Samanta, D.; Maity, S.; Das, D. A Chemodosimetric Approach for Fluorimetric Detection of Hg2+ Ions by Trinuclear Zn (II)/Cd (II) Schiff Base Complex: First Case of Intermediate Trapping in a Chemodosimetric Approach. *Inorg. Chem.* **2020**, *59*, 9014−9028.

(25) (a) Orioli, P.; Cini, R.; Donati, D.; Mangani, S. Crystal and molecular structure of the ternary complex bis [(adenosine 5′-triphosphato)(2, 2′-bipyridine) zinc (II)] tetrahydrate. *J. Am. Chem. Soc.* **1981**, *103*, 4446−4452. (b) Harding, M. M.; Cole, S. J. The crystal structure of di (histidino) zinc pentahydrate. *Acta Crystallogr.* **1963**, *16*, 643−650. (c) Kretsinger, R. H.; Cotton, F. A.; Bryan, R. F. The crystal and molecular structure of di-(l-histidine)-zinc (II) dihydrate. *Acta Crystallogr.* **1963**, *16*, 651−657. (d) Rawle, S. C.; Clarke, A. J.; Moore, P.; Alcock, N. W. Ligands designed to impose tetrahedral co-ordination: a convenient route to aminoethyl and aminopropyl pendant arm derivatives of 1, 5, 9-triazacyclododecane. *J. Chem. Soc., Dalton Trans.* **1992**, *18*, 2755−2757. (e) Charette, A. B.; Marcoux, J. F.; Bélanger-Gariépy, F. X-ray Crystal Structure of a Zinc Carbenoid Cyclopropanating Reagent: The IZnCH2I⊙ 18-crown-6 and Benzo-18-crown-6 Complexes. *J. Am. Chem. Soc.* **1996**, *118*, 6792−6793.

(26) Coxall, R. A.; Harris, S. G.; Henderson, D. K.; Parsons, S.; Tasker, P. A.; Winpenny, R. E. Inter-ligand reactions: in situ formation of new polydentate ligands. *J. Chem. Soc., Dalton Trans.* **2000**, *14*, 2349−2356.

(27) (a) Bourhis, L. J.; Dolomanov, O. V.; Gildea, R. J.; Howard, J. A. K.; Puschmann, H. The anatomy of a comprehensive constrained, restrained refinement program for the modern computing environment - Olex2 dissected. *Acta Crystallogr. A* **2015**, *71*, 59−75. (b) Sheldrick, G. M. SHELXT - Integrated space-group and crystal-structure determination. *Acta Crystallogr. A* **2015**, *71*, 3−8.

(28) Dolomanov, O. V.; Bourhis, L. J.; Gildea, R. J.; Howard, J. A. K.; Puschmann, H. OLEX2: a complete structure solution, refinement and analysis program. *J. Appl. Crystallogr.* **2009**, *42*, 339−341.

(29) Sheldrick, G. M. Crystal structure refinement with SHELXL. *Acta Crystallogr. C* **2015**, *71*, 3−8.

(30) Miertuš, S.; Scrocco, E.; Tomasi, J. Electrostatic Interaction of a Solute with a Continuum. A Direct Utilization of ab initio Molecular Potentials for the Prevision of Solvent Effects. *Chem. Phys.* **1981**, *55*, 117−129.

(31) (a) Wachters, A. J. H. Gaussian basis set for molecular wave functions containing third-row atoms. *J. Chem. Phys.* **1970**, *52*, 1033. (b) Hay, P. J. Gaussian basis sets for molecular calculations − representation of 3D orbitals in transition-metal atoms. *J. Chem. Phys.* **1977**, *66*, 4377−4384. (c) McLean, A. D.; Chandler, G. S. Contracted Gaussian-basis sets for molecular calculations. 1. 2nd row atoms, Z = 11−18. *J. Chem. Phys.* **1980**, *72*, 5639−5648. (d) Krishnan, R.; Binkley, J. S.; Seeger, R.; Pople, J. A. Self-Consistent Molecular Orbital Methods. 20. Basis set for correlated wave-functions. *J. Chem. Phys.* **1980**, *72*, 650−654.

(32) Frisch, M. J.; Trucks, G. W.; Schlegel, H. B.et al.*Gaussian 09*, revision C.01; Gaussian, Inc.: Wallingford, CT, 2010.

https://doi.org/10.1021/acsomega.1c05673
ACS Omega 2022, 7, 1090−1099